Volume 18, Issue 2, 182428 (1-20)

Majlesi Journal of Electrical Engineering (MJEE)

https://dx.doi.org/10.57647/j.mjee.2024.1802.28

Dynamic reconfiguration of the distribution systems with load duration curve (LDC) model for reducing the losses and improving the voltage profile

Sana Sadeghi, Alireza Jahangiri*, Ahmad Ghaderi Shamim

Department of Electrical Engineering, Hamedan Branch, Islamic Azad University, Hamedan, Iran.

***Corresponding author:** a.jahangiri@iauh.ac.ir

Original Research

Received:
13 December 2023
Revised:
21 January 2024
Accepted:
11 March 2024
Published online:
11 May 2024

Abstract:
Distribution systems pose a significant challenge within the power grid, primarily due to their high current, low voltage, and comparatively high ohmic resistance compared to transmission and sub-transmission systems. This results in substantial power losses, necessitating the need for effective mitigation strategies. To address this issue, a wide range of methods and algorithms have been proposed and continuously developed. Over the past half-century, reconfiguring the distribution network has emerged as a cost-effective and straightforward approach to reduce distribution losses. Distribution system reconfiguration has been extensively studied, with each study aiming to achieve distinct objectives. Additionally, numerous studies have explored the dynamics of distribution system reconfiguration, evaluating and comparing various approaches. This study comprehensively assesses both static and dynamic methods of reconfiguring distribution systems and introduces a novel dynamic reconfiguration technique. Unlike traditional methods that rely on real-time or hourly load models, this approach utilizes a load model to address the dynamic reconfiguration problem. Simulations were conducted on the well-established IEEE 33-bus test system, employing MATLAB software in conjunction with a genetic algorithm to minimize losses and optimize voltage profiles. Based on the simulation results, this novel dynamic reconfiguration method demonstrated superior performance compared to previously employed methods. It effectively reduced power losses and enhanced the voltage profile, demonstrating its potential for improving the overall efficiency of distribution systems.

Keywords: Loss reduction; Network reconfiguration; Distribution system; Genetic algorithm; Voltage profile; Load duration curve; Capacitor; Static; Dynamic

1. Introduction

Urban distribution networks, typically constructed as a mesh structure, operate in a radial topology. Distribution network reconfiguration (DNR) involves opening normally closed switches (sectionalizing switches) and closing normally open switches (tie switches). These operations can be controlled manually or automatically using remote control switches. With the appropriate telecommunication infrastructure, remote control of switch statuses is possible. Smart networks, with their quick and accurate reconfiguration abilities, enable efficient utilization of network equipment. Distribution lines exhibit higher power losses compared to transmission lines due to their higher voltage-to-current ratio, resulting in greater impedance. These power losses, operating costs, and voltage profiles are interconnected. DNR aims to minimize power losses during normal operations, particularly in power systems with heavy loads. Additional objectives have emerged, including improving power quality, enhancing voltage safety margins, boosting reliability, expanding line capacity, balancing loads, integrating distributed generation, accelerating service restoration, and prompting rapid recovery [1]. Two primary methods exist for reconfiguring distribution networks, independent of the specific objectives: dynamic distribution network reconfiguration (DDNR) and static distribution network reconfiguration (SDNR). SDNR concentrates on data and constraints about a particular time frame, employing optimization techniques to determine the optimal operational structure. In distribution networks, bus loads fluctuate over time. DDNR ensures reliable, stable, and safe system operation. Indeed, DDNR specifically addresses variable loads. The optimal location and size of devices such as capacitors, Flexible AC Transmission Systems (FACTS), and distributed generation are determined using a variety of optimization methods [2–4]. This study investigates the impact of reconfiguration on distribution network performance by considering shunt capacitor allocation. The modeling of load changes and their effects on the DNR are also explored. The DNR problem was first proposed in [5]. In [6], an advanced SDNR approach, characterized by its dynamic nature, was introduced for network reconfiguration. Unlike traditional SDNR, which assumes a fixed load, this enhanced method employs a variable topology, allowing for timely switch adjustments based on real-time operating conditions. This dynamic approach considers various factors that impact network performance, including load fluctuations, generation variability, uncertain resource availability, market dynamics, switching time constraints, and climate change effects. As a result, the network's performance can be accurately assessed. However, DDNR is computationally more demanding and complex than SDNR [7, 8]. Pioneering work in 1975 introduced classical optimization techniques as efficient tools for addressing the DNR issue [5]. Due to the limitations of classical optimization methods, heuristics methods were introduced as a solution strategy to address the DNR problem. Subsequently, with the advancement of heuristic performance in DNR applications, meta-heuristic approaches were introduced. In [9], the dynamic DNR problem was addressed using BD and B & B algorithms. However, the BD method's accuracy was found to be compromised due to the load-flow equations employed. Additionally, the paper did not compare the efficiency of the proposed method to other online reconfiguration techniques. [10] presents an extended, fast decoupled power-flow method that exhibits significantly lower computational time compared to conventional methods. However, the proposed method's efficiency diminishes in distribution networks characterized by high ohmic resistance-to-reactance ratios. [11] and [12] demonstrate the application of GAMS to solve the multi-objective SDSR problem incorporating demand response. [13] employs an approximate dynamic planning method to restrict DG and shed. [14] utilizes a mathematical modeling language to address the SDNR problem. While methods [15] and [14] produce shorter optimized configurations compared to other mathematical techniques, they are not scalable to large distribution systems. Recently, [16] introduced a novel heuristic based on the Lagrange relaxation method to tackle the DDNR problem. However, linear approximations can limit the accuracy of the obtained solutions in large-scale distribution systems. To address the SDNR problem with DGs, a simple exploration method was developed in [17]. The proposed method successfully reduced power losses and enhanced the rapid voltage stability index. Additionally, [18] introduced a vector shift operation to minimize distribution losses with DG deployment. This algorithm circumvents computationally intensive load-flow calculations by employing power vectors and resistance values. However, linear approximations can limit the accuracy of the obtained solutions in large-scale distribution systems. To address the SDNR problem with DGs, a simple exploration method was developed in [17]. The proposed method successfully reduced power losses and enhanced the rapid voltage stability index. Additionally, [18] introduced a vector shift operation to minimize distribution losses with DG deployment. This algorithm circumvents computationally intensive load-flow calculations by employing power vectors and resistance values. To tackle the integrated problem of DNR and DG allocation, a hybrid optimization approach combining TLBO and the ε-constraint method was proposed in [19], demonstrating superior performance over PSO. [20] Introduced chaos-disturbed beetle antenna search (CDBAS) to simultaneously minimize power losses, unbalanced loadings, and nodal voltage distortions. A fuzzy-modified PSO was employed in [21] to solve a multi-objective SDNR problem, utilizing the Kruskal algorithm for efficient network reconfiguration. The Kruskal algorithm's ability to generate radial topologies without loop evaluation makes it an efficient tool for network reconfiguration. In [22], an enhanced Cuckoo Search Algorithm (CSA) was introduced to tackle a multi-objective SDNR problem incorporating DG and DR. A novel voltage stability constraint for the SDNR problem was proposed in [23], which effectively reduces network losses by considering switched capacitor banks and DGs. The model's results demonstrate the impact of DG output fluctuations on bus voltage. Additionally, [24] addressed both the DNR problem and distributed expansion planning simultaneously. [25] Optimized reactive power losses in SDNRs to reduce distribution system loading limitations. In [26], shunt capacitor banks, voltage regulators, and tap changers were explored as dynamic state control (DSC) control devices in PV-based DG units to minimize energy losses. In this article, load modeling was not addressed. This led [27] to propose the $N-1$ probability criterion for the SDNR problem, aiming to minimize power loss and enhance network security. Later, [28] proposed an SDNR formulation that incorporated power-flow controllers. To conclude, [38] presented a DDNR that leverages renewable energy and energy storage systems to enhance network performance. In conclusion, minimizing power losses and preventing energy waste in distribution networks have significant technical and economic ramifications. Therefore, it is crucial to investigate optimization techniques that effectively reduce losses and costs. This can be accomplished by methods such as reconfiguring and optimizing the allocation of capacitors. For instance, in [29] through a comparative analysis of the cuckoo and cultural algorithms, researchers have addressed the optimal reconfiguration of the smart distribution network in the presence of shunt capacitors, achieving loss reduction and voltage profile improvement. The [30] research proposed the multi-objective optimal allocation of renewable distributed generation and shunt capacitors in the distribution system utilizing corona virus herd optimization techniques. The objective of the study was to attain technical benefits, reduce the total electricity cost, and enhance greenhouse safety. The article [31] presents a methodology for optimizing energy systems in a distribution micro-grid through the application of particle swarm optimization. The approach addresses the optimal production planning of concurrent production systems while considering the loss of electric energy transmission associated with these systems to the grid bus. The article establishes a correlation between the development of optimal load distribution methodology systems and the supply of electrical or thermal load. The proposed algorithm's advantages are demonstrated through numerical studies and comparisons. However, similar to prior articles, load modeling is not employed in this study. The calculations are based on peak load rather than incorporating load modeling into the analysis.[32] Increased integration of distributed generation resources, such as wind power and solar photovoltaic units, into distribution systems necessitates a thorough examination of their impact on the operational reliability of these systems. This paper introduces the concept of multi-objective dynamic feeder reconfiguration as an efficient approach to establish an energy management schedule in the distribution grid. The primary focus is on evaluating and optimizing the reliability of distribution systems in the presence of diverse distributed generation resources. In [33], the authors propose a revised Pareto local search strategy for optimizing the deployment of distributed generation (DG) units and capacitor banks. To curtail the search space and identify Pareto solutions, a novel combination method, comprising Pareto charts and weighting functions, is employed. In [34], the article introduces a network reconfiguration technique for balanced distribution networks, employing Multi-Verse Optimization (MVO) to optimize both total system resistive losses and reduce emissions through step-by-step switching. It is important to note that this study focuses solely on solving the static reconfiguration problem, and there is no mention of incorporating capacitors or load modeling in the analysis. In addition, through a comprehensive review of relevant studies, it has been established that incorporating shunt capacitors (SCs) can effectively reduce power losses and enhance voltage profile. However, neglecting the careful determination of appropriate SC size and placement can lead to detrimental consequences, such as increased power losses, voltage dips, and potential instability. Dynamic reconfiguration has emerged as a novel approach with diverse objectives in the field of distribution network optimization [35]. However, it is crucial to consider the potential cost associated with frequent switching in dynamic reconfiguration. Indeed, excessive switching can lead to significant economic burdens. Therefore, minimizing switching events is essential for efficient network management. As mentioned in the article [36, 37], this challenge has been addressed to some extent, yet it still demands a substantial amount of computational effort. In this study, we have leveraged the load model to optimize dynamic reconfiguration while simultaneously optimizing the allocation of SCs. This holistic approach aims to achieve a synergistic combination of reduced system losses and improved voltage profile stability. Table 1 summarizes the findings of the previous studies and compares them with the proposed method.

2. Problem formulation

Optimized reconfiguration and capacitor allocation methodologies are introduced to improve the effectiveness of distribution networks. Minimizing power losses and enhancing voltage profiles are the principal objectives. To achieve these goals, switches' open/close states are modified through reconfiguration. By analyzing load patterns, the study seeks to minimize active power losses and voltage deviations. The objective function is described below:

$$\text{Minimize}\, f = P_{R,Loss} + VD \tag{1}$$

In this context, $P_{R,Loss}$, represents the cumulative amount of power loss, whereas VD represents the deviation in voltage at a particular bus. Following is a method for calculating the total active power loss:

$$P_{R,Loss} = \sum_{j=1}^{n} R_j * \left(\frac{P_j^2 + Q_j^2}{V_j^2}\right) \tag{2}$$

'n' indicates how many lines are there. There are three variables, R_j, P_j , and Q_j, which represent line resistance,

Table 1. A comparison between the proposed method and some literature.

Ref	CS allocation	Loss reduction	Voltage improvement	Load modeling	SDNR	DDNR
[29]	✓	✓	✓	-	-	-
[30]	✓	✓	✓	-	-	-
[31]	-	✓	-	-	-	-
[32]	✓	✓	-	-	-	-
[33]	✓	✓	✓	-	-	-
[34]	-	✓	-	-	✓	-
[35]	-	✓	✓	-	✓	-
[36]	-	✓	-	-	-	✓
[37]	-	✓	✓	-	-	✓
Proposed method	✓	✓	✓	✓	✓	✓

active and reactive power flow, respectively. R_j represents the voltage of the 'j-th' bus. It is possible to express the voltage deviation as follows, using Equation (3):

$$VD = |1 - V_j| \tag{3}$$

It represents the voltage of the 'j-th' bus in pu. The reconfiguration will minimize the VD closer to zero and improve the network's voltage stability and performance.

3. Limitations

Distribution network reconfiguration should be accompanied by power flow analysis to determine bus voltages, power losses, and branch currents for each proposed configuration. The objective function, however, has certain limitations.

3.1 Bus voltage and current of branches

To ensure the feasibility of a reconfiguration, permissible ranges for bus and branch voltages and currents must be adhered to. These limitations are as follows:

$$V_{\min} \le V_i \le V_{\max} \quad i = 1, 2, \ldots, N_{\text{Bus}} \tag{4}$$

$$I_{\min} \le I_i \le I_{\max} \quad i = 1, 2, \ldots, N_{Br} \tag{5}$$

There are N_{Bus} buses and N_{Br} branches.

3.2 Number and size of capacitors

The use of capacitors is limited for technical and economic reasons. In this study, the number N_c and size Q_c of the capacitors were as follows:

$$1 \le N_c \le 4 \tag{6}$$

$$300\,\text{KVAR} \le Q_c \le 3000\,\text{KVAR} \tag{7}$$

Also:

$$Q_c^T \le Q_L^T \tag{8}$$

In this equation, Q_c^T indicates the total reactive power of capacitor and Q_L^T indicates the total reactive load. (Both in KVAR).

3.3 Radial network verification

In this section, a radial network verification algorithm is presented. The matrix below illustrates the status of switches, indicating whether they are in an open or closed state.

$$M = \begin{bmatrix} Tie_1\, Tie_2 \ldots\ldots Tie_N \\ Sw_1\, Sw_2 \ldots\ldots Sw_N \end{bmatrix}_{2*N} \tag{9}$$

Suppose there are N tie switches, and the state of each switch is Tie_j, i.e., (Open = 0; Close = 1), and the number of closed switches is Sw_j . Each network comprises several loops due to the closure of all switches and the presence of a single open link. Closing this link results in the formation of a loop. It is imperative to open one of the switches within that loop to preserve the radial nature of the network. N is the number of open switches in the network that can be converted to closed switches, and Sw_j is the number of closed switches in the desired loop. Consider the following M-matrix as an example.

$$M = \begin{bmatrix} 01001 \\ 86972 \end{bmatrix}_{2*N} \tag{10}$$

In the following control matrix, it can be seen that the open switches in the first, third, and fourth loops must remain unchanged while the switches in the second and fifth loops must be closed. From the closed switches, the sixth and second switches were opened in order to maintain the radial state of the system.

4. Solution for load flow

This study has employed a direct load flow method [29]. A sample radial distribution network is depicted in Figure 1 to illustrate the direct load distribution method. In Figure 1, it can be seen that I_1, I_2, I_3, I_4, I_5, and I_6 represent the current flowing through the loads corresponding to each bus while the current of the branches is represented by B_1, B_2, B_3, B_4

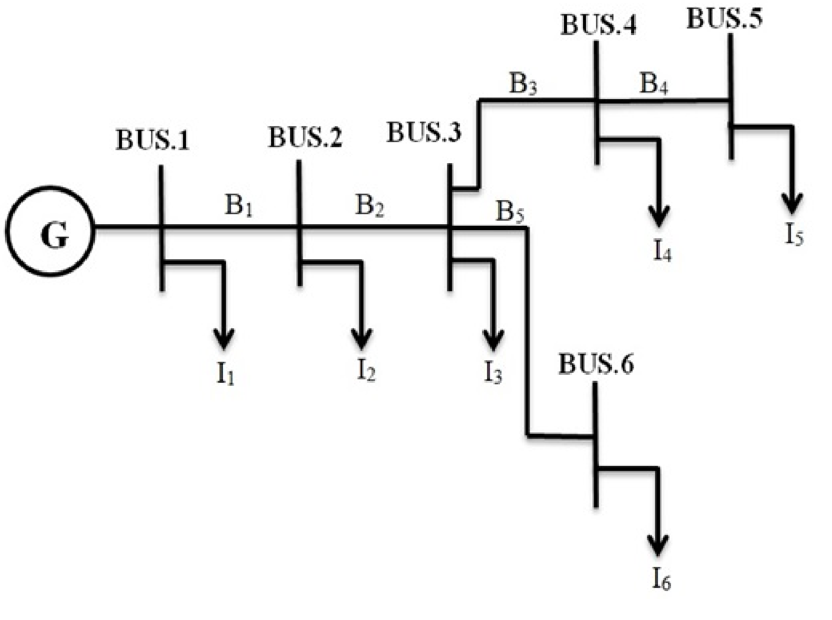

Figure 1. A simple radial distribution.

and B_5, respectively.
The relationship between the currents of branches and loads can be expressed in the following formula:

$$\begin{bmatrix} B_1 \\ B_2 \\ B_3 \\ B_4 \\ B_5 \end{bmatrix} = \begin{bmatrix} 1 & 1 & 1 & 1 & 1 \\ 0 & 1 & 1 & 1 & 1 \\ 0 & 0 & 1 & 1 & 0 \\ 0 & 0 & 0 & 1 & 0 \\ 0 & 0 & 0 & 0 & 1 \end{bmatrix} \begin{bmatrix} I_2 \\ I_3 \\ I_4 \\ I_5 \\ I_6 \end{bmatrix} \tag{11}$$

Equation (11) can be expressed as:

$$[B] = [BIBC]\,[I_i] \tag{12}$$

The following equation can be derived if the impedance between branches i and j is $Z_{ij} = Z_{ji}$:

$$\begin{bmatrix} V_1 - V_2 \\ V_1 - V_3 \\ V_1 - V_4 \\ V_1 - V_5 \\ V_1 - V_6 \end{bmatrix} = \begin{bmatrix} z_{12} & 0 & 0 & 0 & 0 \\ z_{12} & z_{13} & 0 & 0 & 0 \\ z_{12} & z_{23} & z_{34} & 0 & 0 \\ z_{12} & z_{23} & z_{34} & z_{45} & 0 \\ z_{12} & z_{23} & 0 & 0 & z_{36} \end{bmatrix} \begin{bmatrix} B_1 \\ B_2 \\ B_3 \\ B_4 \\ B_5 \end{bmatrix} \tag{13}$$

Matrix Equation (13) can be expressed as follows:

$$[\Delta V] = [BCBV]\,[B] \tag{14}$$

Based on the topological arrangement of distribution systems, the *BIBC* and *BCBV* matrices are constructed. These results can be derived from Equations (12) and (14):

$$[\Delta V] = [BCBV]\,[BIBC]\,[I_i] \tag{15}$$

$$[\Delta V] = [DLF]\,[I_i] \tag{16}$$

where:

$$[DLF] = [BCBV]\,[BIBC] \tag{17}$$

The DLF matrix serves as a representation of the correlation between deviations in bus voltage and load currents within radial distribution systems.

5. Load modeling

It is crucial to acknowledge that during the operation of a distribution network, the load fluctuates and is not constant. Consequently, as the load varies over time, the system's output also changes. Network structures that function optimally at one point in time may not be optimal at another due to these dynamic variations. In the dynamic state of the distribution network, planning and adjusting the operation of the distribution network necessitates the consideration of both the time factor and the network mode [39]. The reconfiguration is affected by changes in the load. DDNR targets a load that varies over time. Because of the variable nature of the load over time and the importance of dynamic reconfiguration of the distribution system, many articles have addressed the issue of hourly and daily reconfiguration [40]. Nevertheless, it is not imperative to address this problem on an hourly basis. Hourly reconfiguration involves consecutive network changes and extensive switching, incurring substantial costs. In this study, instead of employing a series of hourly intervals, we divided the duration of the day into multiple periods and reconfigured the distribution system accordingly. An example of a load curve is shown in Figure 2.
Over 24 hours, Figure 2 shows the load varying. As discussed in previous sections, partitioning the day into distinct periods instead of relying on hourly intervals offers a more effective approach to dynamic reconfiguration. This study employs two methods for dividing the load curve into time periods. A detailed discussion of these techniques is presented as follows.

5.1 Experimental method (EM)

Figure 2 illustrates variations in subscriber consumption over the 24 hours. During certain hours, consumption is low, while for a few hours, it remains at an average level. There are also times when the load is heavy. Consequently, the load curve is categorized into three parts: light, balanced, and peak. Figure 3 shows the experimental method. For all three time periods of peak load, balanced load, and light load, the reconfiguration was performed separately. This is the static reconfiguration method. Typically, static distribution network reconfiguration is evaluated for a specific time point. Moreover, peak load conditions are frequently employed as the decision-making criteria. Ultimately, the optimal mode is determined based on the outcomes of all three stages.

5.2 Spotting method (SM)

Selecting the boundaries between the periods of peak load, balanced load, and light load in the experimental method may be done arbitrarily, leading to potential inaccuracies. Thus, in this study, the spotting method was described as follows:

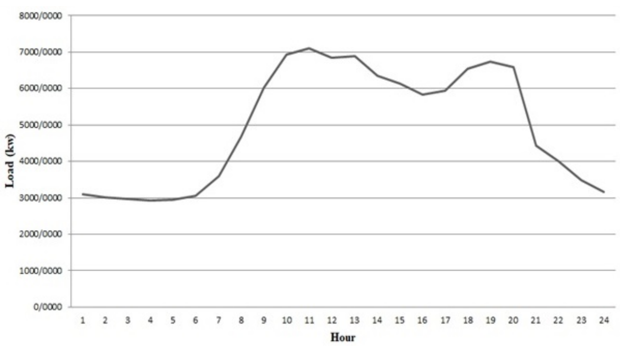

Figure 2. Load curve of IEEE 33 bus

Figure 3. Load duration curve (LDC) of IEEE 33 bus

I. A load curve can be divided into segments with no change, rising loads, or falling loads.
II. The boundaries between these areas were specified, and the load was assumed to be β.
III. The difference between the two points before and after β is calculated and referred to as ΔP.
IV. If ΔP is greater than β, the two regions must be divided into three regions, and the preceding steps must be repeated. Otherwise, the division is correct.
Based on the spotting method, Figure 4 shows the load curve division for the IEEE 33 bus test system.

For all five periods of the spotting method, reconfiguration was carried out individually. In the final stage, the most optimal mode will be determined based on the results obtained from all five stages.

6. Genetic algorithm

In the Genetic Algorithm (GA), the simulation of biological evolution is employed to address both constrained and unconstrained optimization issues. The process involves continuously updating a population of individual solutions. To produce children for the next generation, the GA randomly selects individuals from the current population and uses them as parents. The population evolves toward an optimal solution as successive generations pass. The GA excels in solving problems that may not be well-suited for traditional optimization algorithms. Specifically, it is effective in addressing issues associated with discontinuous, stochastic, or highly nonlinear objective functions. Natural selection, the driving force of evolution, operates by favoring individuals with advantageous traits, ensuring their genetic material is passed on to the next generation. These fitter individuals produce offspring that inherit their beneficial qualities, making them better equipped to thrive and reproduce, further perpetuating the cycle of adaptation and improvement. At the end of this process, the fittest generation will emerge. It is possible to apply this notion to a search problem. The best solutions to a problem are selected from a set of solutions. A genetic algorithm has five steps.

6.1 Initial population

The process begins with a population of individuals, where each individual represents a solution to the problem at hand. The genes within each individual constitute a set of parameters that define its characteristics or variables. Chromosomes are formed by joining genes into a string (solution). A genetic algorithm represents an individual's genes as a string based on an alphabet. Binary values (strings of 1s and 0s) are usually used. Genes are encoded on chromosomes. As a result of entering the network data, the genetic algorithm program generates different randomly selected solutions that present different switch statuses and capacitor allocations. A single random solution is shown in Figure 5. Therefore, different network configurations are initiated randomly.

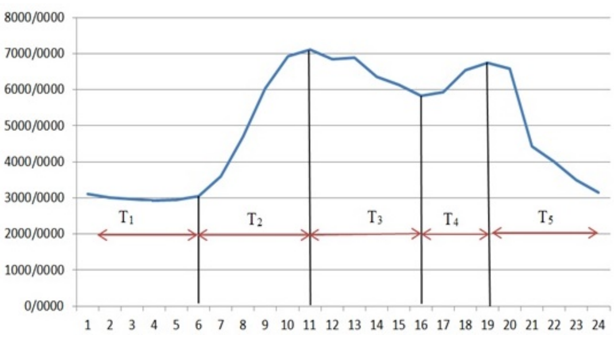

Figure 4. LDC division by spotting method

6.2 Initial population

The assessment of individuals' fitness is based on their ability to outperform their peers. Each individual is assigned a fitness score, and these scores play a critical role in selecting individuals for the reproduction process.

6.3 Selection

The selection process plays a crucial role in the genetic algorithm by identifying and selecting individuals with higher fitness scores to serve as parents for the next generation. This strategic selection enhances the probability of producing offspring with even better fitness, gradually guiding the algorithm towards more optimal solutions.

6.4 Crossover

Genetic algorithms hinge on crossover as a pivotal step. For every pair of parents chosen to mate, a random crossover point is determined within their genes. For instance, considering the crossover point in Figure 6 to be 3, the genes are exchanged or combined at that specific point to generate offspring.
Children are generated through the exchange of genes between parents until a crossover point is reached. This iterative process results in the birth of a new generation of children, as depicted in Figure 7.

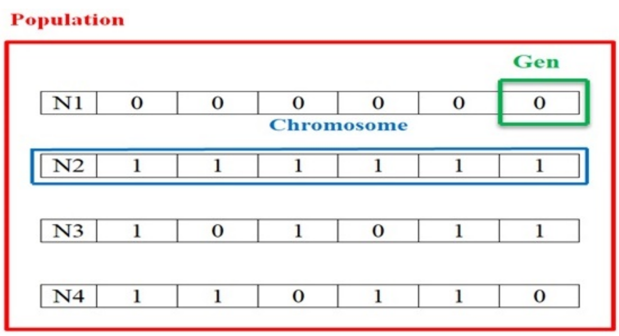

Figure 5. A single random solution

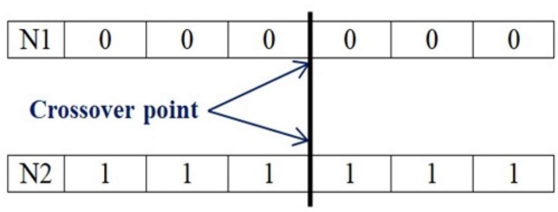

Figure 6. Crossover point

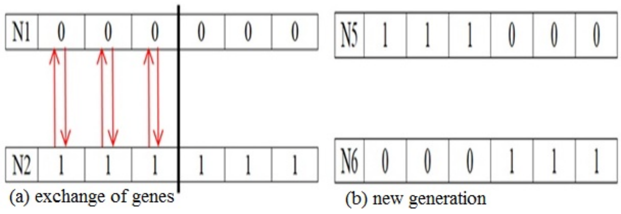

Figure 7. Crossover and a new generation

6.5 Mutation

In newborns, specific genes undergo mutation with a low random probability. In other words, certain bits of the bit string may change from "0" to "1" or vice versa. The mutation is introduced to maintain diversity within the population and prevent premature convergence, ensuring that the genetic algorithm explores a broader solution space.

The simulation process is illustrated in Figure 8. Data about bus, branch, and switch status were entered as part of the second step of optimization. GA parameters such as generation, population, mutation probability, and crossover probability are also specified. Subsequently, random populations are generated. To formulate the objective function, it is necessary to define the search space as well as the end stages of the process. An individual with high-performance parameters was selected from the newly created population at the sixth stage. The population is then sorted so that the fittest individuals appear at the top. In order to complete the steps, the steps are repeated until all constraints have been satisfied.

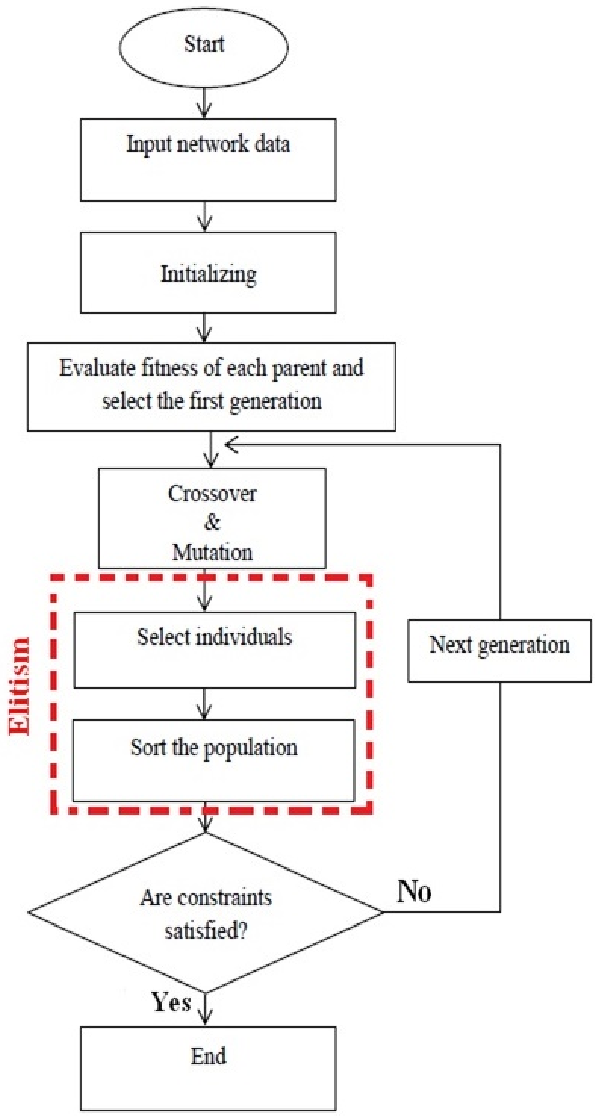

Figure 8. Distribution system reconfiguration and SC allocation flowchart based on the GA algorithm.

7. Results of the simulation

This article undertakes a comparative analysis of two primary optimization approaches: various combinations of reconfiguration and SC allocation. To minimize power loss and voltage deviation, the GA algorithm is applied to solve the network reconfiguration and capacitor allocation problem. MATLAB software was utilized to simulate six scenarios using the IEEE 33 Bus System to assess and verify performance. These are the scenarios:
The first scenario: Base case.
The second scenario: Just network reconfiguration.
The third scenario: Just capacitor allocation.
The fourth scenario: Allocation of capacitors after reconfiguration.
The fifth scenario: Network reconfiguration after allocation of capacitors.
The sixth scenario: Network reconfiguration and capacitor allocation simultaneously.
In all six of the above cases, both the (EM) and (SM) methods will be simulated, and at the end, the most appropriate method of dividing the time will be determined.

7.1 Base Cace

The base case, representing the system without capacitors or network reconfiguration, is considered to establish the initial power losses and bus voltage. This scenario serves as a benchmark for comparison with other cases. Figure 9 shows a single-line diagram of the 33-bus system. According to Figure 9, the 33-bus system consists of 32 sectionalizing switches and five tie switches. The numbering of the sectionalizing switches ranges from 1 to 32, whereas the numbering of the tie switches ranges from 33 to 37. Simulation results are shown in Table 2.

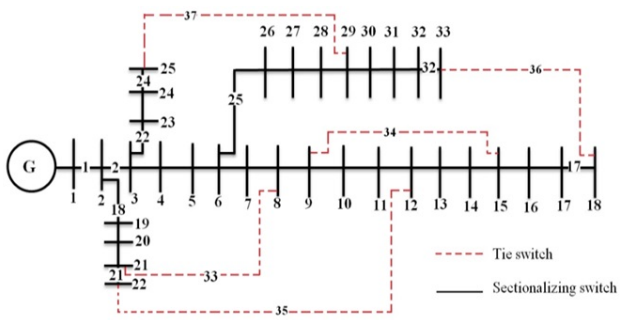

Figure 9. Single-line diagram of the 33-bus system

Table 2. Analyses of the first scenario.

Method	Power Loss (kW)	Minimum Bus Voltage (pu)	Tie Switches
EM			33,34,35,36,37
Peak Load	575.36	0.85	-
Balanced Load	202.67	0.91	-
Light Load	47.07	0.95	-
SM			33,34,35,36,37
Period 1	38817.50	0.31	-
Period 2	32610.41	0.30	-
Period 3	36227.23	0.30	-
Period 4	36275.00	0.28	-
Period 5	30655.34	0.34	-

7.2 Just network reconfiguration

This case focuses solely on network reconfiguration to minimize power losses and enhance the voltage profile without incorporating capacitors. Tables 3 and 4 present the simulation results for this particular scenario.
Considering the results in Tables 2, 3 and 4, if the goal is to reduce distribution system losses with distribution system reconfiguration, more loss reduction can be achieved with (SM) modeling than (EM) modeling. In addition, peak load decisions can be more effective than balanced and light loads, and (SM) load modeling is more useful if the goal is to improve the voltage profile of the distribution network. ((SM) method's 30% increase compared to (EM) method's 10% increase) Figures 10 and 11 illustrate the changes in the voltage profile using the (EM) and (SM) methods, respectively.

7.3 Just capacitor placement

This scenario assumes that the only way to reduce losses and improve the voltage profile is through capacitor addition to the distribution system. It is not necessary to make any changes to the system configuration. Tables 5 and 6 display the simulation results for this specific scenario.
Based on Tables 2, 5 and 6, it appears that the (SM) method is more suitable for improving voltage profile and reducing losses than the (EM) method. Furthermore, if the decision-making basis is the fifth period, the most significant reduction in losses (67.36%) is achieved. It is better to place the peak load on a decision-making basis if it is to be modeled (EM), because of the greatest reduction in losses.
Figures 12 and 13 illustrate the changes in the voltage profile obtained using the (EM) and (SM) methods, respectively.

Table 3. Second scenario simulation results for (EM) method.

Load Type	Paramerts	Details
Peak Load	Tie switches	36,34,23,20,10
	Size of the capacitor (KVAR)	-
	Location of the capacitor (Bus No)	-
	Minimum bus voltage (pu)	0.95
	Power losses (kW)	446.43
	Loss reduction (%)	22.40
Balanced Load	Tie switches	36,20,11,8,5
	Size of the capacitor (KVAR)	-
	Location of the capacitor (Bus No)	-
	Minimum bus voltage (pu)	0.95
	Power losses (kW)	200.89
	Loss reduction (%)	0.87
Light Load	Tie switches	33,29,14,10,4
	Size of the capacitor (KVAR)	-
	Location of the capacitor (Bus No)	-
	Minimum bus voltage (pu)	0.97
	Power losses (kW)	45.63
	Loss reduction (%)	3.05

Table 4. Second scenario simulation results for (SM) method.

Load Type	Paramerts	Details
Period 1	Tie switches	34,29,11,7,4
	Size of the capacitor (KVAR)	-
	Location of the capacitor (Bus No)	-
	Minimum bus voltage (pu)	0.95
	Power losses (kW)	30299.61
	Loss reduction (%)	21.94
Period 2	Tie switches	37,34,32,9,4
	Size of the capacitor (KVAR)	-
	Location of the capacitor (Bus No)	-
	Minimum bus voltage (pu)	0.95
	Power losses (kW)	32608.78
	Loss reduction (%)	0.005
Period 3	Tie switches	34,32,25,10,3
	Size of the capacitor (KVAR)	-
	Location of the capacitor (Bus No)	-
	Minimum bus voltage (pu)	0.95
	Power losses (kW)	36225.34
	Loss reduction (%)	0.005
Period 4	Tie switches	36,25,10,8,5
	Size of the capacitor (KVAR)	-
	Location of the capacitor (Bus No)	-
	Minimum bus voltage (pu)	0.95
	Power losses (kW)	22103.16
	Loss reduction (%)	39.06
Period 5	Tie switches	31,25,20,14,8
	Size of the capacitor (KVAR)	-
	Location of the capacitor (Bus No)	-
	Minimum bus voltage (pu)	0.95
	Power losses (kW)	30653.46
	Loss reduction (%)	0.006

Table 5. Third scenario simulation results for (EM) method.

Load Type	Paramerts	Details
Peak Load	Tie switches	33,34,35,36,37
	Size of the capacitor (KVAR)	1200,300,300,300
	Location of the capacitor (Bus No)	3,2,6,33
	Minimum bus voltage (pu)	0.95
	Power losses (kW)	268.14
	Loss reduction (%)	53.39
Balanced Load	Tie switches	33,34,35,36,37
	Size of the capacitor (KVAR)	300,300,600,2400
	Location of the capacitor (Bus No)	4,6,33,19
	Minimum bus voltage (pu)	0.95
	Power losses (kW)	134.69
	Loss reduction (%)	33.54
Light Load	Tie switches	33,34,35,36,37
	Size of the capacitor (KVAR)	600,300,1200,600
	Location of the capacitor (Bus No)	21,31,6,2
	Minimum bus voltage (pu)	0.97
	Power losses (kW)	42.87
	Loss reduction (%)	8.92

Table 6. Second scenario simulation results for (SM) method.

Load Type	Paraments	Details
Period 1	Tie switches	33,34,35,36,37
	Size of the capacitor (KVAR)	3000,2700,3000,3000
	Location of the capacitor (Bus No)	13,7,33,12
	Minimum bus voltage (pu)	0.95
	Power losses (kW)	14096.26
	Loss reduction (%)	63.68
Period 2	Tie switches	33,34,35,36,37
	Size of the capacitor (KVAR)	1500,3000,2100,3000
	Location of the capacitor (Bus No)	12,16,33,7
	Minimum bus voltage (pu)	0.95
	Power losses (kW)	11448.11
	Loss reduction (%)	64.89
Period 3	Tie switches	33,34,35,36,37
	Size of the capacitor (KVAR)	3000,1500,3000,3000
	Location of the capacitor (Bus No)	12,33,31,6
	Minimum bus voltage (pu)	0.95
	Power losses (kW)	13572.64
	Loss reduction (%)	62.53
Period 4	Tie switches	33,34,35,36,37
	Size of the capacitor (KVAR)	2400,3000,3000,3000
	Location of the capacitor (Bus No)	30,33,12,6
	Minimum bus voltage (pu)	0.95
	Power losses (kW)	12761.90
	Loss reduction (%)	64.81
Period 5	Tie switches	33,34,35,36,37
	Size of the capacitor (KVAR)	3000,1200,3000,3000
	Location of the capacitor (Bus No)	12,24,33,14
	Minimum bus voltage (pu)	0.95
	Power losses (kW)	10003.64
	Loss reduction (%)	67.36

Table 7. Fourth scenario simulation results for (EM) method.

Load Type	Paraments	Details
Peak Load	Tie switches	36,34,23,20,10
	Size of the capacitor (KVAR)	3000,1200,300,300
	Location of the capacitor (Bus No)	11,33,30,10
	Minimum bus voltage (pu)	0.95
	Power losses (kW)	263.71
	Loss reduction (%)	54.16
Balanced Load	Tie switches	37,33,21,14,6
	Size of the capacitor (KVAR)	1500,300,3000,1200
	Location of the capacitor (Bus No)	2,33,11,5
	Minimum bus voltage (pu)	0.95
	Power losses (kW)	130.73
	Loss reduction (%)	35.49
Light Load	Tie switches	33,29,14,10,4
	Size of the capacitor (KVAR)	3000,1200,300,1800
	Location of the capacitor (Bus No)	7,14,33,21
	Minimum bus voltage (pu)	0.99
	Power losses (kW)	38.43
	Loss reduction (%)	18.35

Table 8. Fourth scenario simulation results for (SM) method.

Load Type	Paraments	Details
Period 1	Tie switches	34,29,11,7,4
	Size of the capacitor (KVAR)	2400,3000,3000,300
	Location of the capacitor (Bus No)	7,33,8,13
	Minimum bus voltage (pu)	0.96
	Power losses (kW)	9039.40
	Loss reduction (%)	76.71
Period 2	Tie switches	37,34,32,9,4
	Size of the capacitor (KVAR)	2700,3000,2100,3000
	Location of the capacitor (Bus No)	27,33,28,13
	Minimum bus voltage (pu)	0.95
	Power losses (kW)	11443.80
	Loss reduction (%)	64.90
Period 3	Tie switches	34,32,25,10,3
	Size of the capacitor (KVAR)	300,3000,3000,3000
	Location of the capacitor (Bus No)	3,25,33,21
	Minimum bus voltage (pu)	0.95
	Power losses (kW)	13568.26
	Loss reduction (%)	66.22
Period 4	Tie switches	37,27,12,8,6
	Size of the capacitor (KVAR)	1200,3000,1500,1800
	Location of the capacitor (Bus No)	9,20,33,24
	Minimum bus voltage (pu)	0.95
	Power losses (kW)	9762.53
	Loss reduction (%)	73.08
Period 5	Tie switches	31,25,20,14,8
	Size of the capacitor (KVAR)	1200,300,3000,2400
	Location of the capacitor (Bus No)	13,28,33,9
	Minimum bus voltage (pu)	0.95
	Power losses (kW)	9999.52
	Loss reduction (%)	70.59

7.4 Allocation of capacitors after reconfiguration

In this scenario, network reconfiguration is initially performed, followed by the placement of capacitors to further enhance optimization outcomes. Tables 7 and 8 display the simulation results for this specific scenario.
Based on Tables 2, 7 and 8 it appears that the (SM) method is more suitable for improving the voltage profile and reducing losses than the (EM) method. Furthermore, if the decision-making basis was the first period, the most significant reduction in losses (76.71%) would be achieved. It is better to place the peak load on a decision-making basis if it is to be modeled (EM) because of the greatest reduction in losses.
Figures 14 and 15 illustrate the changes in the voltage profile obtained using the (EM) and (SM) methods, respectively.

7.5 Network reconfiguration after allocation of capacitors

As in the previous scenario, the situation is similar in this case. On the other hand, a capacitor was initially installed in the network and reconfigured. To determine the most optimal case, would it be better to install the capacitor first and then reconfigure the system, or Inverse?
Tables 9 and 10 present the simulation results for this specific scenario.
Based on Tables 2, 9 and 10, it appears that the (SM) method is more suitable for improving the voltage profile and reducing losses than the (EM) method. Furthermore, if the decision-making basis is the fifth period, the most significant reduction in losses (83.22%) is achieved. It is better to place the peak load on a decision-making basis if it is to be modeled (EM) because of the greatest reduction in losses. Figures 16 and 17 illustrate the changes in the voltage profile obtained using the (EM) and (SM) methods, respectively.

7.6 Network reconfiguration and capacitor allocation simultaneously

In this scenario, the installation of capacitors coincides with distribution system reconfiguration.
Tables 11 and 12 depict simulation results for this particular scenario.
Upon analysis of Tables 2, 11, and 12, it is evident that the (SM) method proves to be more effective in enhancing the voltage profile and minimizing losses compared to the (EM) method. Furthermore, if the decision-making basis is

Table 9. Fifth scenario simulation results for (EM) method.

Load Type	Paramerts	Details
Peak Load	Tie switches	32,22,12,9,7
	Size of the capacitor (KVAR)	1200,300,300,300
	Location of the capacitor (Bus No)	3,2,6,33
	Minimum bus voltage (pu)	0.95
	Power losses (kW)	262.06
	Loss reduction (%)	54.45
Balanced Load	Tie switches	32,25,18,10,8
	Size of the capacitor (KVAR)	300,300,600,2400
	Location of the capacitor (Bus No)	4,6,33,19
	Minimum bus voltage (pu)	0.95
	Power losses (kW)	129.42
	Loss reduction (%)	36.14
Light Load	Tie switches	34,31,2710,6
	Size of the capacitor (KVAR)	600,300,1200,600
	Location of the capacitor (Bus No)	21,31,6,2
	Minimum bus voltage (pu)	0.98
	Power losses (kW)	37.09
	Loss reduction (%)	21.20

Table 10. Fifth scenario results for (SM) method.

Load Type	Paramerts	Details
Period 1	Tie switches	37,35,27,11,6
	Size of the capacitor (KVAR)	3000,2700,3000,3000
	Location of the capacitor (Bus No)	13,7,33,12
	Minimum bus voltage (pu)	0.95
	Power losses (kW)	9037.91
	Loss reduction (%)	76.71
Period 2	Tie switches	36,33,10,8,4
	Size of the capacitor (KVAR)	1500,300-,2100,3000
	Location of the capacitor (Bus No)	12,16,33,7
	Minimum bus voltage (pu)	0.95
	Power losses (kW)	10230.94
	Loss reduction (%)	68.62
Period 3	Tie switches	37,15,11,8,5
	Size of the capacitor (KVAR)	3000,1500,3000,3000
	Location of the capacitor (Bus No)	12,33,31,6
	Minimum bus voltage (pu)	0.95
	Power losses (kW)	6133.79
	Loss reduction (%)	83.06
Period 4	Tie switches	31,25,14,8,5
	Size of the capacitor (KVAR)	2400,3000,3000,3000
	Location of the capacitor (Bus No)	30,33,12,6
	Minimum bus voltage (pu)	0.95
	Power losses (kW)	9760.66
	Loss reduction (%)	73.09
Period 5	Tie switches	37,14,11,7,5
	Size of the capacitor (KVAR)	3000,1200,3000,3000
	Location of the capacitor (Bus No)	12,24,33,14
	Minimum bus voltage (pu)	0.95
	Power losses (kW)	5143.84
	Loss reduction (%)	83.22

Table 11. Sixth scenario simulation results for (EM) method.

Load Type	Paramerts	Details
Peak Load	Tie switches	33,28,20,13,7
	Size of the capacitor (KVAR)	300,2100,3000,1200
	Location of the capacitor (Bus No)	33,4,21,14
	Minimum bus voltage (pu)	0.95
	Power losses (kW)	248.46
	Loss reduction (%)	56.81
Balanced Load	Tie switches	37,35,29,14,6
	Size of the capacitor (KVAR)	3000,300,1200,1800
	Location of the capacitor (Bus No)	19,31,3,20
	Minimum bus voltage (pu)	0.95
	Power losses (kW)	104.99
	Loss reduction (%)	48.19
Light Load	Tie switches	23,17,9,8,5
	Size of the capacitor (KVAR)	3000,300,600,3000
	Location of the capacitor (Bus No)	11,16,33,18
	Minimum bus voltage (pu)	0.98
	Power losses (kW)	27.04
	Loss reduction (%)	42.55

Table 12. Sixth scenario results for (SM) method.

Load Type	Paramerts	Details
Period 1	Tie switches	33,31,24,11,5
	Size of the capacitor (KVAR)	3000,3000,300,300
	Location of the capacitor (Bus No)	15,33,4,23
	Minimum bus voltage (pu)	0.95
	Power losses (kW)	9034.09
	Loss reduction (%)	76.72
Period 2	Tie switches	29,21,10,6,5
	Size of the capacitor (KVAR)	3000,3000,2700,3000
	Location of the capacitor (Bus No)	11,22,33,17
	Minimum bus voltage (pu)	0.95
	Power losses (kW)	5478.89
	Loss reduction (%)	83.19
Period 3	Tie switches	33,21,13,83
	Size of the capacitor (KVAR)	2100,1200,3000,3000
	Location of the capacitor (Bus No)	33,3,25,30
	Minimum bus voltage (pu)	0.95
	Power losses (kW)	3787.41
	Loss reduction (%)	89.54
Period 4	Tie switches	33,27,19,11,8
	Size of the capacitor (KVAR)	2400,300,3000,300
	Location of the capacitor (Bus No)	33,4,20,22
	Minimum bus voltage (pu)	0.95
	Power losses (kW)	9756.26
	Loss reduction (%)	73.10
Period 5	Tie switches	37,29,13,9,7
	Size of the capacitor (KVAR)	3000,300,300,2100
	Location of the capacitor (Bus No)	15,16,33,14
	Minimum bus voltage (pu)	0.95
	Power losses (kW)	5140.02
	Loss reduction (%)	83.23

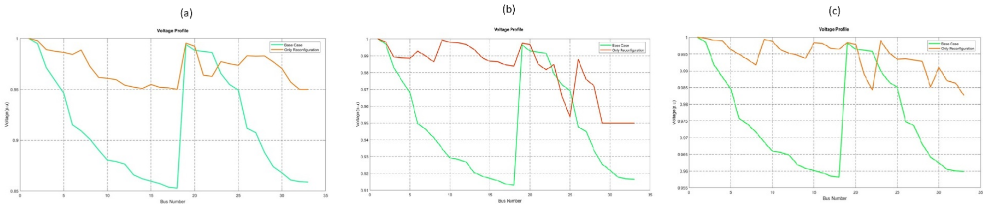

Figure 10. Changes in voltage profile by (EM), a) peak load, b) balanced load, c) light load.

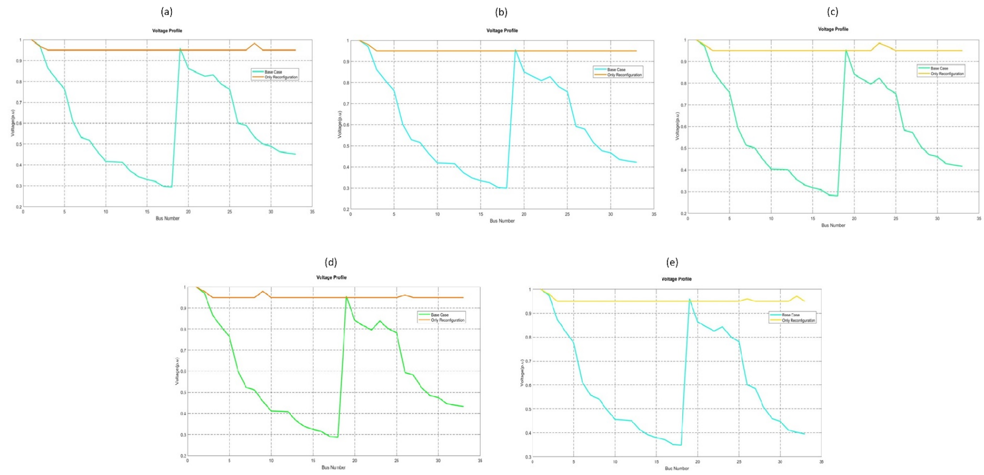

Figure 11. Changes in voltage profile by (SM), a) period T1, b) period T2, c) period T3, d) period T4, e) period T5.

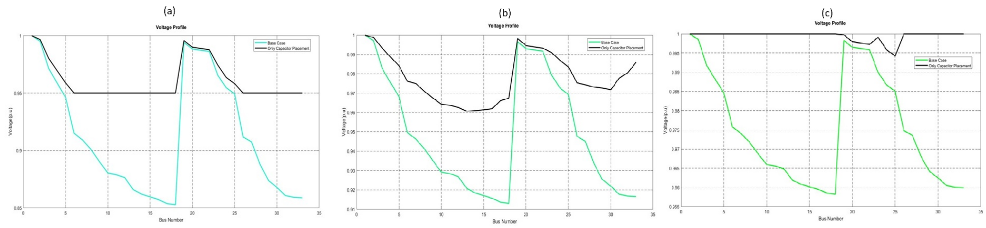

Figure 12. Changes in voltage profile by (EM), a) peak load, b) balanced load, c) light load.

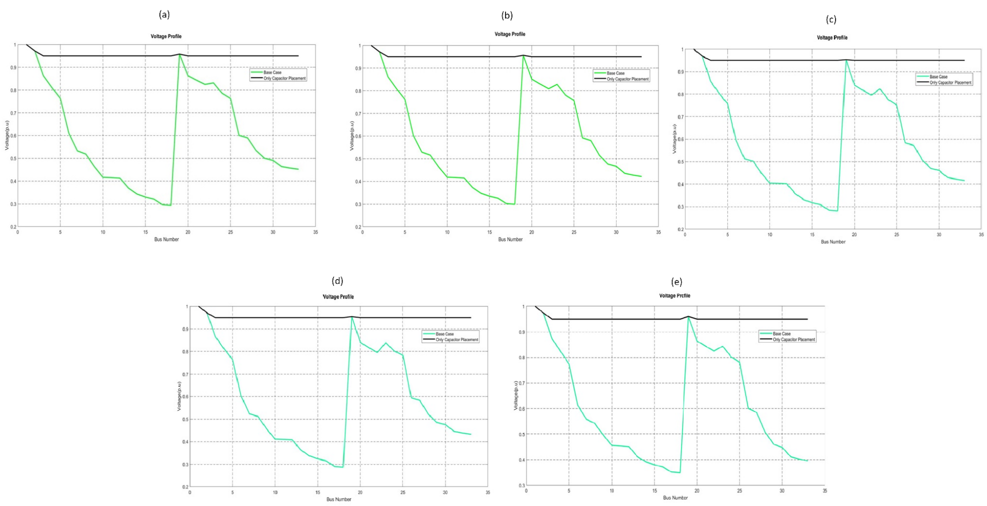

Figure 13. Changes in voltage profile by (SM), a) period T1, b) period T2, c) period T3, d) period T4, e) period T5.

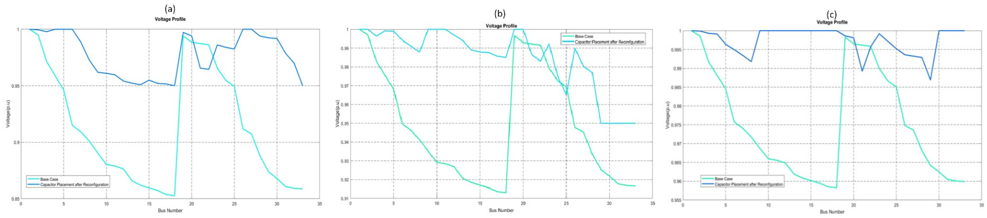

Figure 14. Changes in voltage profile by (EM), a) peak load, b) balanced load, c) light load.

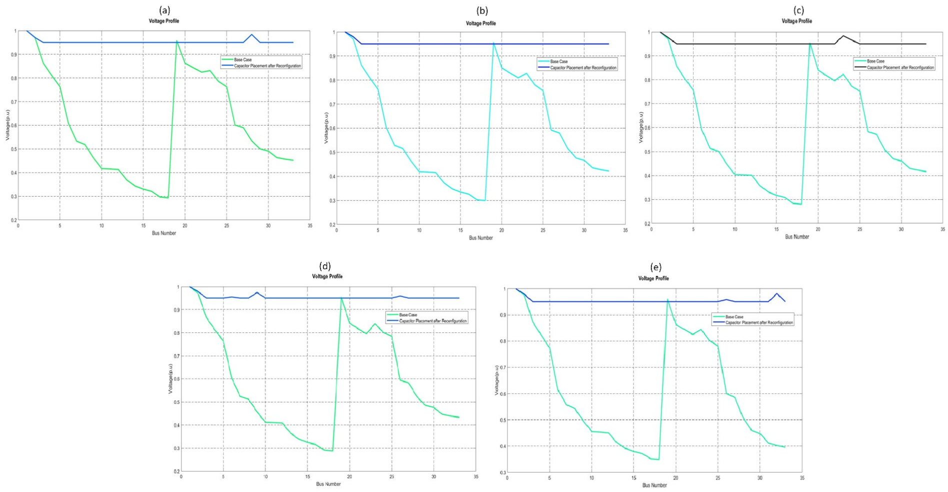

Figure 15. Changes in voltage profile by (SM), a) period T1, b) period T2, c) period T3, d) period T4, e) period T5.

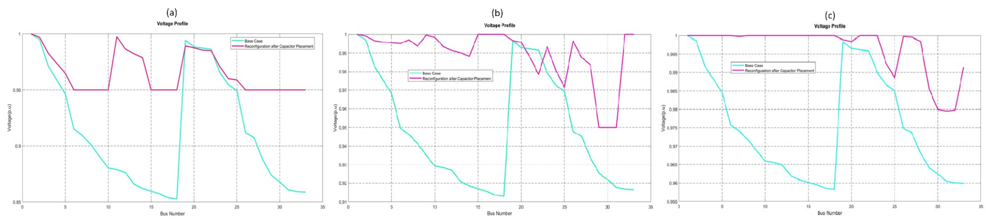

Figure 16. Changes in voltage profile by (EM), a) peak load, b) balanced load, c) light load.

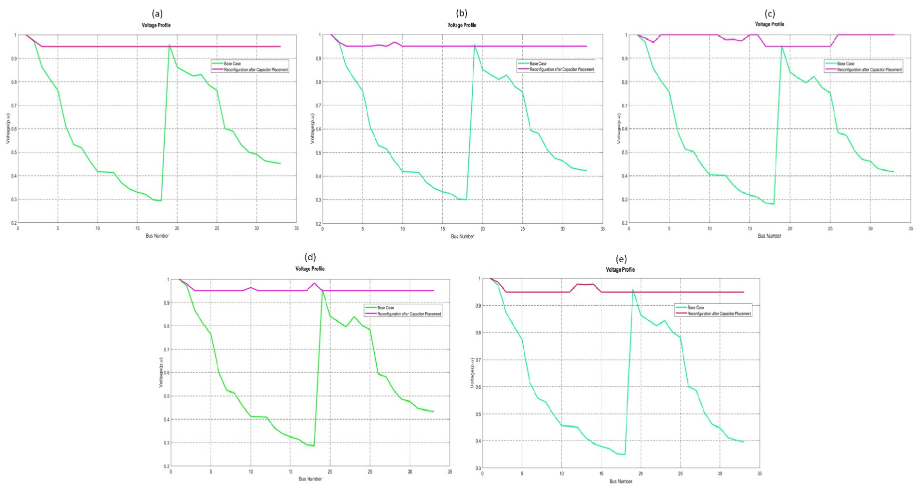

Figure 17. Changes in voltage profile by (SM), a) period T1, b) period T2, c) period T3, d) period T4, e) period T5.

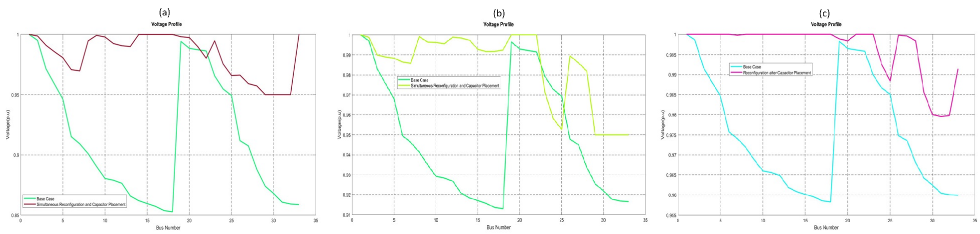

Figure 18. Changes in voltage profile by (EM), a) peak load, b) balanced load, c) light load.

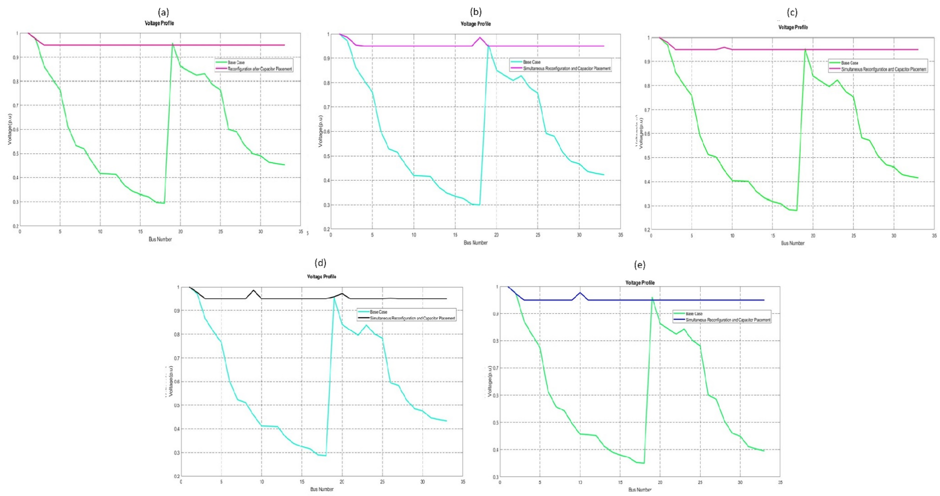

Figure 19. Changes in voltage profile by (SM), a) period T1, b) period T2, c) period T3, d) period T4, e) period T5.

in the third period, the most significant reduction in losses (89.54%) is achieved. It is better to place the peak load on a decision-making basis if it is to be modeled (EM) because it will reduce loss and improve the voltage profile. Based on the simulation results, scenario 6 showed the most significant loss reduction and voltage profile improvement. Figures 18 and 19 depict the variations in voltage profile observed under the (EM) and (SM) methods, respectively.
Figure 20 summarizes the simulation results of the (EM) method.
As shown in Figure 20, the peak load exhibited the highest percentage of loss reduction in all the cases. The balanced load, followed by the light load, exhibited the highest percentage of loss reduction. Furthermore, the lowest percentage of loss reduction was associated with only reconfiguration, whereas the highest percentage was associated with simultaneous reconfiguration and capacitor placement.
Figure 21 summarizes the simulation results of the (SM) method.
As depicted in Figure 21, the third period demonstrated the most significant loss reduction. Moreover, standalone reconfiguration produced the lowest percentage of loss reduction, whereas simultaneous reconfiguration and capacitor placement attained the highest loss reduction percentage.
Figure 22 contrasts the minimum and maximum percentages of loss reduction between the two methods, (EM) and (SM).
Figure 23 shows a comparison of the highest voltage increase. As shown in Figure 23, the maximum voltage range increase of the (SM) is 70.83%. (From 0.28 pu to 0.96 pu). It is also significant to note that the voltage range of the (EM) has increased by 14.42%. (0.85 pu to 0.99 pu).

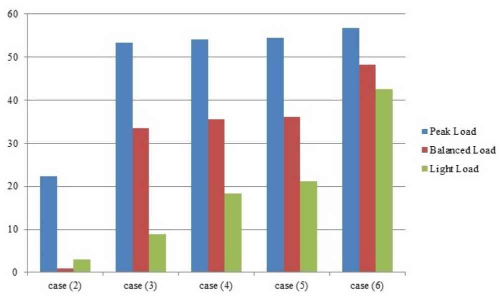

Figure 20. Summary of the simulation results of the (EM) method.

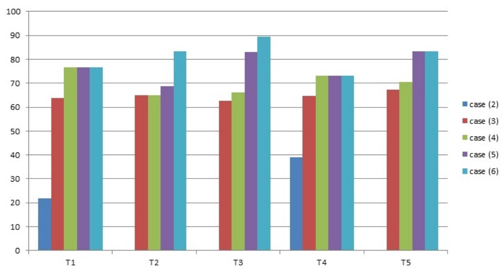

Figure 21. Summary of the simulation results of the (SM) method.

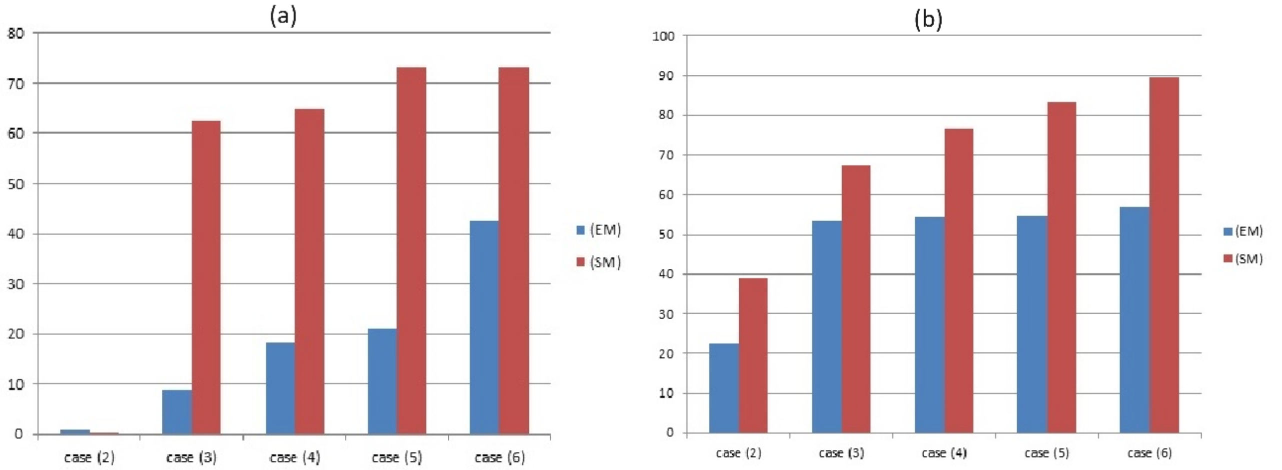

Figure 22. Comparison of the lowest and highest loss reduction percentages between (EM) and (SM). a) lowest percentage b) highest percentage.

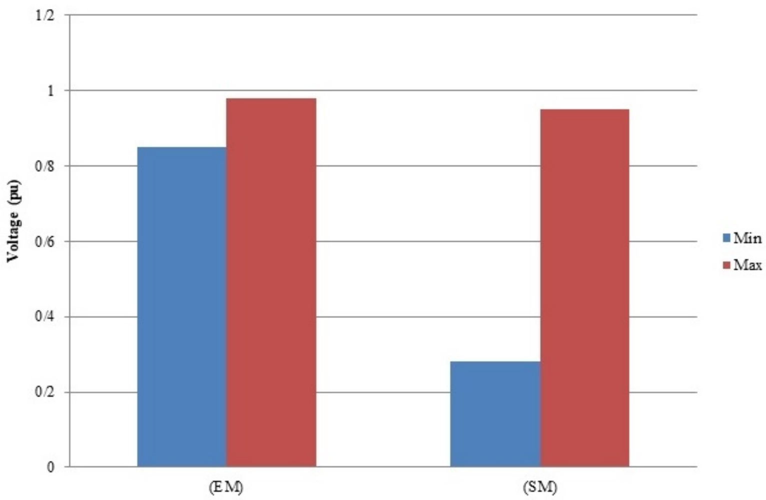

Figure 23. Comparison of the highest voltage increase.

8. Conclusion

This study introduces a novel dynamic reconfiguration method for mitigating power losses, enhancing voltage profile quality, and optimizing capacitor allocation. Utilizing the Genetic Algorithm and the IEEE 33 Bus test system in MATLAB software, simulations were carried out to ascertain that, along with the reduction in losses, there was a substantial improvement in the voltage profile. In static reconfiguration, only the current state of the network is considered, which may not satisfy all the requirements of the network in the future. As a result, the challenge of dynamic reconfiguration was introduced, inevitably giving rise to issues such as successive switching and increased costs. This study introduced a novel dynamic reconfiguration method. In this method, rather than conducting reconfiguration hourly, 24 h was divided into several periods during which capacitor allocation and reconfiguration were performed. This method, encompassing the entire 24-hour timeframe, effectively eliminates the need for frequent hourly reconfiguration and the associated challenges of consecutive switching. The simulation results showed that this method performed reasonably well. Both static and dynamic performances were assessed using two load modeling methods (EM) and (SM), and it was found that the (SM) method is more efficient and has a significant impact on voltage profile improvement and loss reduction. Furthermore, it was determined that the combined implementation of capacitor installation and distribution network reconfiguration yielded superior performance outcomes. Simulations revealed that implementing capacitor installation before distribution system reconfiguration resulted in a more substantial reduction in power losses. Simulation findings indicated that the peak load criterion exhibited superior efficacy in static reconfiguration compared to the balanced or light load criterion.

Authors Contributions
All authors have contributed equally to prepare the paper.

Availability of Data and Materials
The data that support the findings of this study are available from the corresponding author upon reasonable request.

Conflict of Interests
The authors declare that they have no known competing financial interests or personal relationships that could have appeared to influence the work reported in this paper.

Open Access

References

[1] N. C. Koutsoukis, D. O. Siagkas, P. S. Georgilakis, and N. D. Hatziargyriou. "**Online reconfiguration of active distribution networks for maximum integration of distributed generation**.". *IEEE Trans. Autom. Sci. Eng.*, 14(2):pp. 437–448, 2017.

[2] P.Kayal and C.K.Chanda. "**A simple and fast approach for allocation and size evaluation of distributed generation**.". *Int. J. Energy Environ. Eng.*, **4** (7), 2013.

[3] S. Lal and A. Laturi. "**Techno-economic analysis of a hybrid mini-grid system for Fiji islands**.". *Int. J. Energy. Environ. Eng.*, **3**(10), 2012.

[4] S.M. Islam. "**Increasing wind energy penetration level using pumped hydro storage in island microgrid system**.". *Int. J. Energy. Environ. Eng.*, 3(9), 2012.

[5] A. Merlin and H. Back. "**Search for a minimal-loss operating spanning tree configuration in an urban power distribution system**.". *Proc. 5th Power Syst. Comput. Conf., London, U.K.*, pages pp. 1–18, 1975.

[6] G. Chang, J. Zrida, and J. D. Birdwell. "**Knowledge-based distribution system analysis and reconfiguration**.". *IEEE Trans. Power Syst.*, 5(3):pp. 744–749, 1990.

[7] Y.-Y. Fu and H.-D. Chiang. "**Toward optimal multi-period network recon-configuration for increasing the hosting capacity of distribution networks**.". *IEEE Trans. Power Del.*, 33(5):pp. 2294–2304, 2018.

[8] R. A. Jabr, I. Dac, and I. Huseinagi. "**Real time optimal reconfiguration of multiphase active distribution networks**.". *IEEE Trans. Smart Grid*, 9(6):pp. 6829–6839, 2018.

[9] Y. Takenobu, N. Yasuda, S. Kawano, S. I. Minato, and Y. Hayashi. "**Evaluation of annual energy loss reduction based on reconfiguration scheduling**.". *IEEE Trans. Smart Grid*, 9(3):pp. 1986–1996, 2018.

[10] A. G. Fonseca, O. L. Tortelli, and E. M. Lourenço. "**Extended fast decoupled power _ow for reconfiguration networks in distribution systems**.". *ET Gener., Transmiss. Distrib.*, 12(22):6033–6040, 2018.

[11] M. A. T. G. Jahani, P. Nazarian, A. Safari, and M. R. Haghifam. "**Multi-objective optimization model for optimal reconfiguration of distribution networks with demand response services**.". *Sustain. Cities Soc.*, 47:pp. 1–11, 2019.

[12] E. Kianmehr, S. Nikkhah, and A. Rabiee. "**Multi-objective stochastic model for joint optimal allocation of DG units and network reconfiguration from DG owner's and DisCo's perspectives**.". *Renew. Energy*, 132:pp. 471–485, 2019.

[13] C. Wang, S. Lei, P. Ju, C. Chen, C. Peng, and Y. Hou. "**MDP-based distribution network reconfiguration with renewable distributed generation: Approximate dynamic programming approach**.". *IEEE Trans. Smart Grid*, 11(4):pp. 3620–3631, 2020.

[14] M. Mahdavi and R. Romero. "**Reconfiguration of radial distribution systems: An efficient mathematical model**.". *IEEE Latin Amer. Trans.*, 19(7):pp. 1172–1181, 2021.

[15] M. Mahdavi, H. H. Alhelou, N. D. Hatziargyriou, and A. Al-Hinai. "**An efficient mathematical model for distribution system reconfiguration using AMPL**.". *IEEE Access*, 9:pp. 79961–79993, 2021.

[16] N. V. Kova£ki, P. M. Vidovi, and A. T. Sari¢. "**Scalable algorithm for the dynamic reconfiguration of the distribution network using the Lagrange relaxation approach**". *Int. J. Elect. Power Energy Syst.*, 94:pp. 188–202, 2018.

[17] K. Jasthi and D. Das. "**Simultaneous distribution system reconfiguration and DG sizing algorithm without load _ow solution**.". *IET Gener., Trans- miss. Distrib*, 12(6):pp. 1303–1313, 2018.

[18] X. Ji, Q. Liu, Y. Yu, S. Fan, and N. Wu. "**Distribution network reconfiguration based on vector shift operation**.". *IET Gener., Transmiss. Distrib.*, 12(13):pp. 3339–3345, 2018.

[19] I. A. Quadri, S. Bhowmick, and D. Joshi. "**Multi- bjective approach to maximize loadability of distribution networks by simultaneous recon-guration and allocation of distributed energy resources**.". *IET Gener., Transmiss. Distrib.*, 12(21):pp. 5700–5712, 2018.

[20] J. Wang, W. Wang, Z. Yuan, H. Wang, and J. Wu. "**A chaos disturbed beetle antennae search algorithm for a multi-objective distribution network reconfiguration considering the variation of load and DG**.". *IEEE Access*, 8:pp. 97392–97407, 2020.

[21] H. Wu, P. Dong, and M. Liu. "**Distribution network reconfiguration for loss reduction and voltage stability with random fuzzy uncertainties of renewable energy generation and load**.". *IEEE Trans. Ind. Informat.*, 16(9):pp. 5655–5666, 2020.

[22] A. Abbasi. "**Investigation of simultaneous effect of demand response and load uncertainty on distribution feeder reconfiguration**.". *IET Gener., Transmiss. Distrib.*, 14(8):pp. 1438–1449, 2020.

[23] Y. Song, Y. Zheng, T. Liu, S. Lei, and D. J. Hill. "**A new formulation of distribution network reconfiguration for reducing the voltage volatility induced by distributed generation**.". *IEEE Trans. Power Syst.*, 35(1):pp. 496–507, 2020.

[24] I. B. Cattani, E. Chaparro, and B. Barán. "**Distribution system operation and expansion planning using network reconfiguration**.". *IEEE Latin Amer. Trans.*, 18(5):pp. 845–852, 2020.

[25] A. Tyagi, A. Verma, and P. R. Bijwe. "**Recongeration for loadability limit enhancement of distribution systems**.". *IET Gener., Transmiss. Dis- trib.*, 12(1):pp. 88–93, 2018.

[26] V. B. Pamshetti, S. Singh, and S. P. Singh. "**Combined impact of network reconfiguration and volt-VAR control devices on energy savings in the presence of distributed generation**.". *IEEE Syst. J.*, 14(1):pp. 995–1006, 2020.

[27] G. Zu, J. Xiao, and K. Sun. "**Distribution network reconfiguration comprehensively considering N_1 security and network loss**.". *IET Gener., Transmiss. Distrib.*, 12(8):pp. 1721–1728, 2018.

[28] Y. Yang, S. Zhang, W. Pei, J. Sun, and Y. Lu. "**Network reconfiguration and operation optimisation of distribution system with flexible DC device**.'. *J. Eng.*, 2019(16):pp. 2401–2404, 2019.

[29] S. Sadeghi, A. Jahangiri, and A. Ghaderi Shamim. "**Optimal reconfiguration of a smart distribution network in the presence of shunt capacitors**.". *Electrical Engineering*, 106:pp. 603–6014, 2023. DOI: https://doi.org/10.1007/s00202-023-01997-y.

[30] O. W. Adebiyi, M. O. Okelola, and S. A. Salimon. "**Multi-objective Optimal Allocation of Renewable Energy Distributed Generations and Shunt Capacitors in Radial Distribution System using Corona Virus Herd Optimization**.". *Majlesi Journal of Electrical Engineering*, 17(3):pp. 145–164, 2023. DOI: https://doi.org/10.30486/mjee.2023.1978728.1068.

[31] W. K. Al-Azzawi et al. "**Optimization of Energy Systems in a Distribution Micro grid: An Application of the Particle Swarm Optimization**.". *Majlesi Journal of Electrical Engineering*, 17(2):pp. 41–46, 2023. DOI: https://doi.org/10.30486/mjee.2023.1987130.1147.

[32] H. Lotfi, A. Nikooei, A. Shojaei, R. Ghazi, and M. B. Naghibi Sistani. "**An Enhanced Evolutionary Algorithm for Providing Energy Management Schedule in the Smart Distribution Network**.". *(in en), Majlesi Journal of Electrical Engineering*, 14(2): pp. 17–23, 2020.

[33] A. Sadighmanesh, M. Sabahi, and M. Zavvari. "**Pareto Local Search Function for Optimal Placement of DG and Capacitors Banks in Distribution Systems**.". *Majlesi Journal of Electrical Engineering*, 15(3):pp. 81–92, 2021. DOI: https://doi.org/10.52547/mjee.15.3.81.

[34] A. V. Reddy, M. Damodar Reddy, and Y. V. Reddy. "**Feeder Reconfiguration of Distribution Systems for Loss Reduction and Emissions Reduction Using MVO Algorithm**.". *(in en), Majlesi Journal of Electrical Engineering*, 12(2):1–8, 2018.

[35] Q. Liu, L. Zhang, X. Ji, and H. Shi. "**Dynamic reconfiguration of distribution network considering the uncertainty of distributed generation and loads**.". *(in English), Frontiers in Energy Research, Original Research*, 11, 2023. DOI: https://doi.org/10.3389/fenrg.2023.1279579.

[36] S. M. Razavi, H. R. Momeni, M. R. Haghifam, and S. Bolouki. "**Multi-Objective Optimization of Distribution Networks via Daily Reconfiguration**.". *IEEE Transactions on Power Delivery*, 37(2):pp. 775–785, 2022. DOI: https://doi.org/10.1109/TPWRD.2021.3070796.

[37] H. Gao, W. Ma, S. He, L. Wang, and J. Liu. "**Time-Segmented Multi-Level Reconfiguration in Distribution Network: A Novel Cloud-Edge Collaboration Framework**.". *IEEE Transactions on Smart Grid*, 13(4):pp. 3319–3322, 2022. DOI: https://doi.org/10.1109/TSG.2022.3156433.

[38] A. Azizivahed, A. Are, S. Ghavidel, M. Shae-Khah, L. Li, J. Zhang, and J. P. S. Catalão. "**Energy management strategy in dynamic distribution network

reconfiguration considering renewable energy resources and storage.". *IEEE Trans. Sustain. Energy*, 11(2):662–673, Apr. 2020.

[39] X. Ji, Z. Yin, Y. Zhang, B. Xu, and et al. "**Real-time autonomous dynamic reconfiguration based on deep learning algorithm for distribution network**.". *Electric. Power Syst. Res.*, **195**:107132, June. 2021.

[40] C. Wang, Y. Xu, and J. Zhang. "**Dynamic Reconfiguration of Distribution Network Based on Symbolization of Time Series of Load**.". *2019 IEEE 3rd International Electrical and Energy Conference (CIEEC), Beijing, China*, :1001–1006, 2019. DOI: https://doi.org/10.1109/CIEEC47146.2019.CIEEC-2019377.